Effect of absorber plate material on the performance of flat plate solar air heater under free convection

Efecto del material de la placa absorbedora en el desempeño de calentadores solares de aire de placa plana (SAH), bajo convección libre

R.C. Salmorán-Salgado^{1‡}, F. J. Moreno-García², J.E. Botello-Álvarez³, B. Ríos-Fuentes⁴, M. Calderón-Ramirez⁵, M. C. Pérez-Pérez⁶, J. M. Gutiérrez-Villalobos⁷, L. Fausto-Castro⁸

¹Tecnológico Nacional de México en Celaya, Programa de Doctorado en Ciencias de la Ingeniería. García Cubas 600 Celaya, Gto. 38010, México.

²Tecnológico Nacional de México en Celaya, Programa de Maestría en Ciencias en Ingeniería Mecatrónica. García Cubas 600 Celaya, Gto. 38010, México.

³Tecnológico Nacional de México en Celaya, Departamento de Ingeniería Bioquímica y Ambiental. García Cubas 600 Celaya, Gto. 38010. México.

⁴Departamento de Ingeniería Agroindustrial, Universidad de Guanajuato, Celaya, 38060, México.

⁵Tecnológico Nacional de México CRODE Celaya, Celaya, 38020, México.

⁶Tecnológico Nacional de México en Celaya, Departamento de Ingeniería Bioquímica y Ambiental. García Cubas 600 Celaya, Gto. 38010, México.

Departamento de Ingeniería Agroindustrial. Universidad de Guanajuato, Celaya, 38060, México.
⁸Departmento de Ingeniería Industrial, Universidad del Sabes, Apaseo El Grande, Guanajuato, 38163, México.
Sent date: January 25, 2025; Accepted: June 23, 2025

Abstract

Solar air heaters (SAH) are an alternative to harness solar energy. In SAH's, a metal plate absorber retains solar radiation to transfer it to the air. The effect of the plate material: aluminum, galvanized steel and carbon steel and the number of sheets on the thermal efficiency of SAH's was evaluated, with an experimental design 32. The analysis shows that the material and the number of sheets have no effect on the thermal efficiency of SAH's. A phenomenological analysis indicates that interfacial heat transport between the black paint film covering the absorber plates, and the air represents the greatest resistance to heat transfer. It is proposed to use covers with better optical properties that increase the surface temperature and the intensity of free convection. *Keywords*: Solar energy, absorber plate, coat of paint.

Resumen

Los calentadores solares de aire (SAH) son una alternativa para aprovechar la energía solar. En los SAH's, un absorbedor de placas metálicas retiene la radiación solar para transferirla al aire. Se evaluó el efecto del material de las placas: aluminio, acero galvanizado y acero al carbón y el número de láminas sobre la eficiencia térmica de los SAH's, con un diseño experimental 32. El análisis muestra que el material y el número de láminas no tienen efecto sobre la eficiencia térmica de los SAH's. Un análisis fenomenológico indica que el transporte de calor interfacial entre la película de pintura negra que cubre las placas absorbentes, y el aire representa la mayor resistencia a la transferencia de calor. Se propone utilizar cubiertas con mejores propiedades ópticas que aumenten la temperatura superficial y la intensidad de la convección libre. *Palabras clave*: Energía solar, placa absorbedora, cubierta de pintura.

[‡]Corresponding author. E-mail: robertosalgado2329@gmail.com; https://doi.org/10.24275/rmiq/IA25513 ISSN:1665-2738, issn-e: 2395-8472

•

1 Introduction

The global temperature increase is expected to exceed 2°C in 2050. To avoid this, it is proposed to leave 60% of gas and oil reserves underground and 90% of coal reserves (Welsby *et al.*, 2021). Countries and companies whose economies and development are based on the use of fossil fuels will find it challenging to comply with these recommendations, so it is necessary to intensify the use of clean energy and make processes more efficient worldwide. Solar thermal energy systems use solar radiation to heat fluids such as air and water, which is an economical and versatile alternative for integration into industrial applications (Schoeneberger *et al.*, 2020).

In 2017, the global food industry consumed 200 EJ (200×10^{18} J); the main forms of energy used are electrical and thermal. Energy consumption per kilogram of finished food product varies from 1.18 to 16.22 MJ. The primary consumption is thermal energy (Ladha-Sabur et al., 2019). Drying consumes between 3.0 and 16 MJ per kg of dried product, and the drying temperature is between 50 and 120 °C (Sanjuán *et al.*, 2014). Solar drying is a practice that uses environmentally available energy. It allows for significant energy savings.

Solar thermal energy allows the integration of conventional and renewable energy sources to meet the thermal demands of certain food processing operations. Hybrid solar dryers are designed to combine solar energy with various types of auxiliary energy, including electric, fossil, renewable photovoltaic, wind, and biomass sources (Kong *et al.*, 2024). Indirect solar dryers employ air preheating through SAH's (Mekhilef *et al.*, 2011). SAH's are rectangular prisms comprising a glass cover and a metal plate with a black painted surface, known as the absorber. Air flows between the two plates, with heating occurring via natural or forced convection. The absorber plate receives solar radiation and transforms it into internal energy, enabling the heating of air from 30°C to 80°C (Kalogirou, 2003).

Solar energy, though intermittent, holds immense potential for the future. It is crucial to devise mechanisms that facilitate the accumulation of solar radiation during days with high insolation, its subsequent controlled storage, and regulated discharge, thereby compensating for unpredictable weather patterns. In their 2020 study Das & Akpinar, (2020) developed a solar drying system that employed a tracking mechanism. The SAH's absorber plate utilized aluminum, which reached temperatures between 51.7°C and 81.7°C. In a study conducted by Mohammed *et al.* (2024), a series of SAH's absorber

surfaces, painted in black and comprising silicon powder, were tested. The surfaces were exposed to solar radiation values of 560 W/m² and temperatures of up to 60°C, demonstrating the promising potential of solar drying technology. Solar radiation impinges upon the absorber plate of the SAH's, thereby increasing its internal energy and raising its surface temperature. The air entering the SAH's is subjected to a rise in temperature due to heat transfer through conduction and convection mechanisms. The thermal efficiency of the SAH's is determined by calculating the ratio between the heat energy gained by the air and the solar energy incident on the absorber plate. It can be seen that a proportion of the energy absorbed by the SAH's is dissipated into the surrounding environment rather than being transferred to the transfer fluid. The elevated percentage of energy loss in SAH's can be attributed to the optical properties of the paint layer, the thermal characteristics of the metal plate, hydrodynamic conditions, and the transport properties of the air in contact with the surface (Singh et al., 2019, Iglesias-Díaz et al. 2011).

The black paint film is the primary active component of an SAH; it is the center of absorption for solar radiation, which is transformed into internal energy and then transferred by conduction to the rear metal plate and into the air through its exposed face. The paint film is formed by a mixture of a polymeric matrix and metal oxides, including copper, cobalt, chromium, and nickel, arranged as dispersed particles or nanoparticles. Techniques have also been used where compounds of the aforementioned metals are electrochemically fixed to the absorber plate, forming dark aggregates with high absorbance (Kumar *et al.*, 2022).

Its high thermal conductivity is the primary criterion for selecting an SAH absorber plate material. Using plates with enhanced thermal properties will result in the generation of equipment with superior performance. In a study conducted by Handoyo et al., (2014), aluminum-based absorber plates were utilized with a surface treatment referred to as "prismatic obstacles," resulting in efficiency values ranging from 0.15 to 0.85. Srivastava et al., (2017) report that implementing fins on aluminum-based absorber plates allows an operating efficiency of approximately 0.338. The selection of absorber plate coatings should be based on their high absorbance and low emissivity coefficients. Kumar et al., (2022) describe a coating formed from nanostructured CuO with an absorbance factor of 0.9 and an emissivity of 0.14.

This study aims to ascertain the impact of three SAH absorber plate materials on thermal efficiency when used aluminum, galvanized steel, and carbon steel in a free convection environment. Three identical SAHs were constructed to ensure that the absorber plates of material different were subjected to identical environmental conditions and equal solar radiation.

2 Methodology

The dimensions of the SAHs are shown in Figure 1a. The prismatic body was constructed of ¾ inch pine wood and was painted with matte black enamel. The bottom was insulated with 1 ½ inch thick pink fiberglass. At the bottom, it has three 2.0 inch diameter holes to allow air inlet; at the top, it has a 4.0 inch diameter hole for air outlet.

The flat absorber plates are made of aluminum, galvanized steel and carbon steel with thicknesses of 1.5, 1.6 and 1.5 mm, respectively. The faces exposed to the sun were coated with matte black enamel. A 5.9 mm thick flat glass was used as a cover. As mentioned before, three identical SAHs were made to expose the absorber plates to the same environmental conditions; for this purpose, a platform was built to support the

SAHs, where the dimensions are shown in Figure 1b and 1c. The platform has an inclination of 30° with respect to the horizontal. The experiments were carried out at the facilities of the TecNM in Celaya (20°32'18"N 100°49'09"W), in May and June 2024, exposing the SAHs from 10:00 to 15:00 hours. The environmental conditions during the experiments were: Temperature (25.4°C - 40.4°C), Humidity (21% - 57%), and Solar radiation (100 W/m²-1390 W/m²).

Air temperatures at the inlet and outlet of the SAHs were measured with J-type thermocouples (Maxim Integrated DS18B20:155 -122°C), where they were recorded on a laptop PC. The air velocity at the inlet of the SAHs was measured with a hot wire anemometer (Hot Wire Traceable Anemometer/Thermometer 4330CC, 0.2-20 m/s). The amount of solar radiation on the SAHs was measured with a solarimeter (TES-1333R, 0-2000 W/m²). Environmental conditions were recorded through a portable weather station placed at the measurement site (Generic, -40-60°C, 20%-90% humidity). A portable thermal camera (FLIR TG165, -25°C-380°C) was used to measure the temperature profiles on the absorber plates.

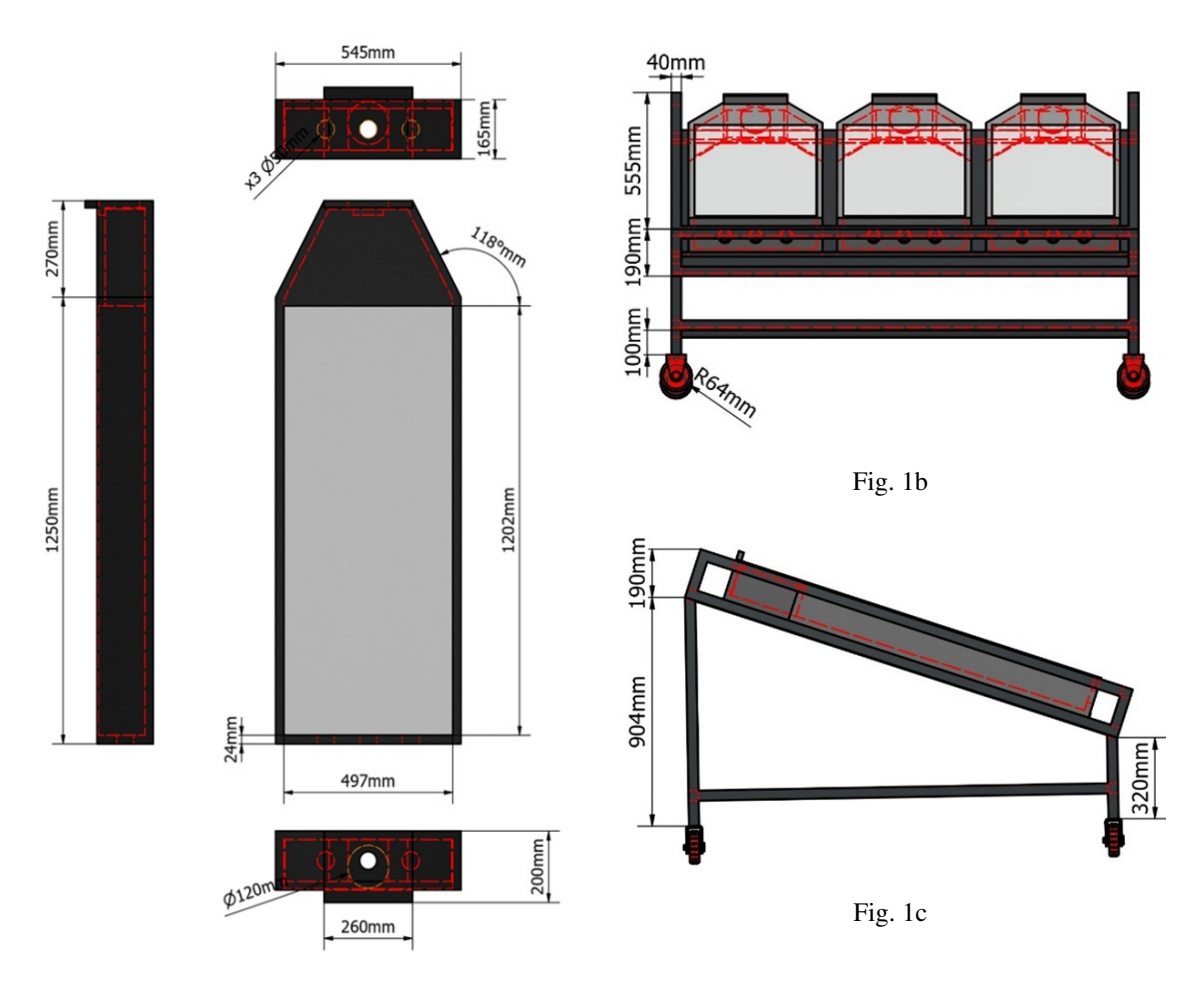


Fig. 1a

www.rmiq.org 3

A 3² experimental design was carried out, where two factors were studied: absorber plate material and number of sheets with three levels, materials: aluminum, galvanized steel, carbon steel and number sheets: 1, 2, 3. In each experiment, absorber plates of different materials were used, placed in each of the SAH's, in order to reduce the effect of uncontrolled environmental conditions on the thermal performance of the SAH's, and the experiments were carried out in triplicate for three continuous days.

To estimate the thermal efficiency η according to Equation 1 (Pardeshi *et al.*, 2024) it is necessary to estimate the mass flow rate of air circulating through the SAH, driven by buoyancy forces, which depend on the axial and transverse differences in air density associated with the local temperatures between the shell and absorber plate.

$$\eta = \frac{\dot{m}C_p(T_{ao} - T_{ai})}{I_{\text{solar}}A_{\text{plate}}} \tag{1}$$

Where m and Cp are the mass flow rate and heat capacity of the air, T_{ao} and T_{ai} are the air inlet and outlet temperatures to the SAHs, I_{solar} is the solar incidence of the air, and A_{plate} is the area of the absorber plate exposed to solar radiation. The air properties (density and heat capacity) were estimated at the average temperature of Tao and Tai, considering the data reported by Green & Southard (2019). For all experiments, the convective heat transfer coefficients were estimated using Equation 2 (Sidebotham, 2015).

$$Nu_{\rm air} = 0.54 Ra^{1/4} \tag{2}$$

This equation is valid for gas mixtures heated on an inclined metal surface. Where Nuair is the Nusselt number for air, using the separation between the absorber plate and the glass cover as the characteristic distance. Ra is the Rayleigh number; this equation is valid for a Ra range of 104–106 10⁴-10⁶ (Sidebotham, 2015).

The experimental data on air temperatures at the outlet of the SAH's, as well as the estimated data on thermal efficiency with different absorber plate materials, were statistically analyzed using "t student" tests to evaluate the hypothesis of equality of means. In the case of temperatures, their dispersion was evaluated by estimating confidence intervals for an α of 0.05, using Excel® tools.

In addition, further experiments were performed as described above, with intermittent operation of continuous exposure to radiation for 40 minutes and then for 20 minutes the SAH's were covered with completely opaque cardboard. During these periods the heating and cooling rates of the air inside the SAH's were calculated.

3 Results

3.1 Thermal efficiencies

Figure 2 presents the temperatures and solar radiation monitored during an experiment for three solar air heaters (SAHs) with absorber plates made of different materials. The average air temperatures at the SAH outlet are shown for the three experiments using one absorber plate; the bars indicate the maximum and minimum temperatures for each measurement. A comparative Student t-test between the experimental data sets for each absorber plate material indicated no significant differences in the average temperatures for SAHs with absorber plates made of different materials.

Figure 3A presents the thermal efficiencies and average solar radiation, along with their specified ranges between the maximum and minimum values, for SAHs with absorber plates of different materials—case (2 sheets). The estimated efficiencies do not exceed 20% despite a temperature increase of nearly 30°C as the air passes over the absorber plates. The low efficiencies are mainly associated with the low mass air flows driven by free convection phenomena. During some experiments, clouds formed, casting shadows over the SAHs and resulting in a substantial decrease in incident solar radiation, as observed in Figure 3B. Under these circumstances, a significant increase in thermal efficiencies occurs because the air continued to heat up, associated with the energy absorbed by the absorber plates and the rest of the SAH body due to radiation exposure prior to the shadows. Under these circumstances, SAHs with aluminum sheets experience higher thermal efficiencies.

Yadav & Bhagoria (2013) mention that smooth plate SAHs have poor performance; the inclusion of fins, posts, roughness, and baffles improves thermal efficiency but also increases friction, pressure drop, and energy expenditure due to the inclusion of blowers. The thermal efficiency with forced convection for SAHs with smooth and rough plates was 19.78-44.26% and 52.51-72.20%.

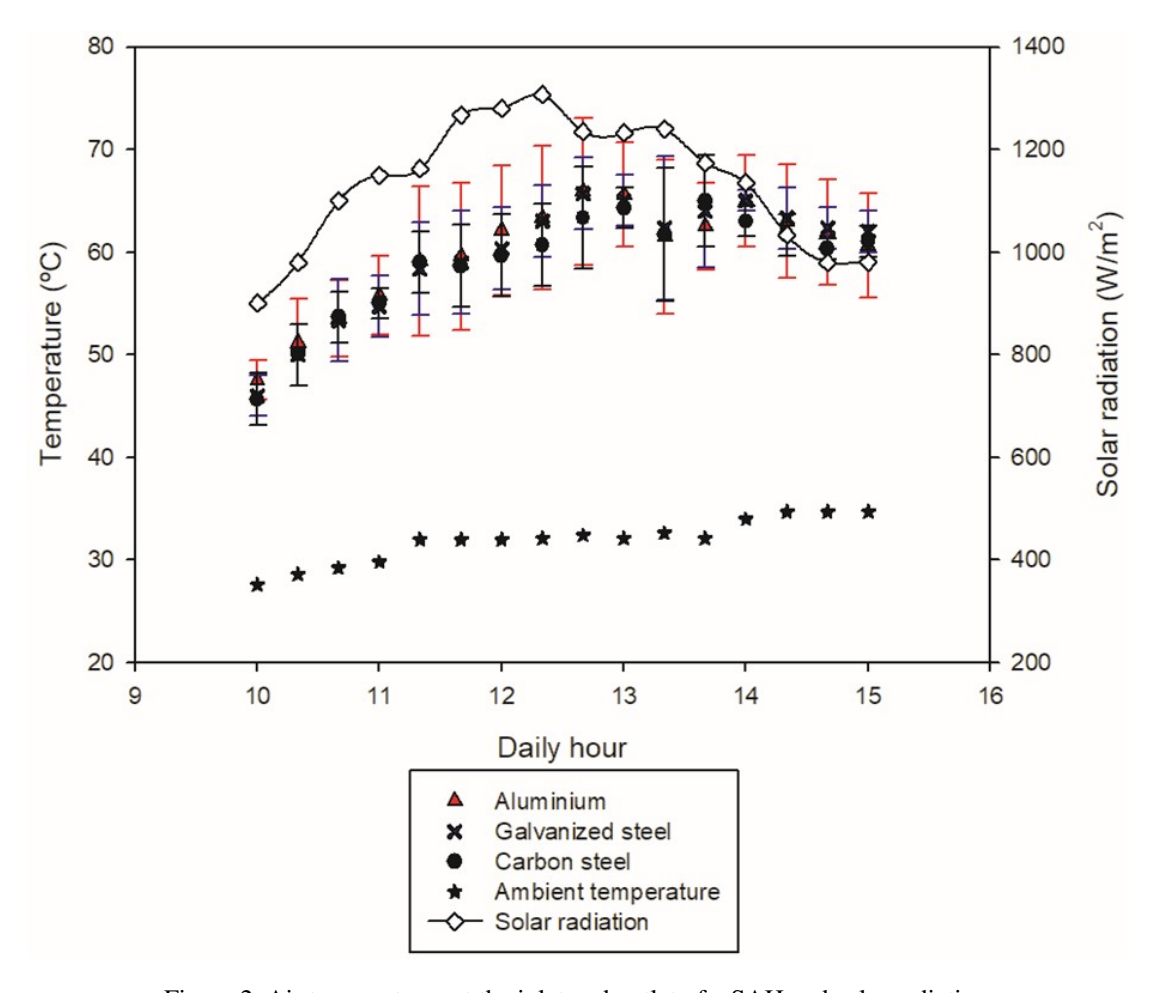


Figure 2. Air temperatures at the inlet and outlet of a SAH and solar radiation. Use of $(1 \ sheet)$.

www.rmiq.org

5

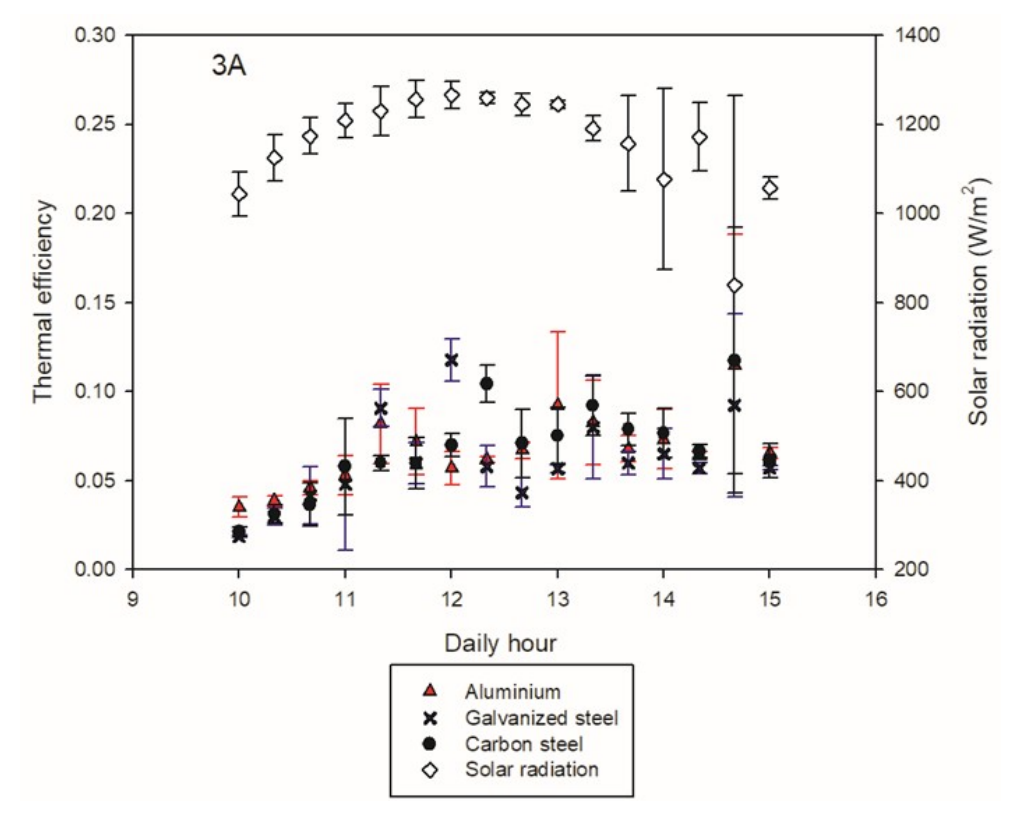


Fig. 3A

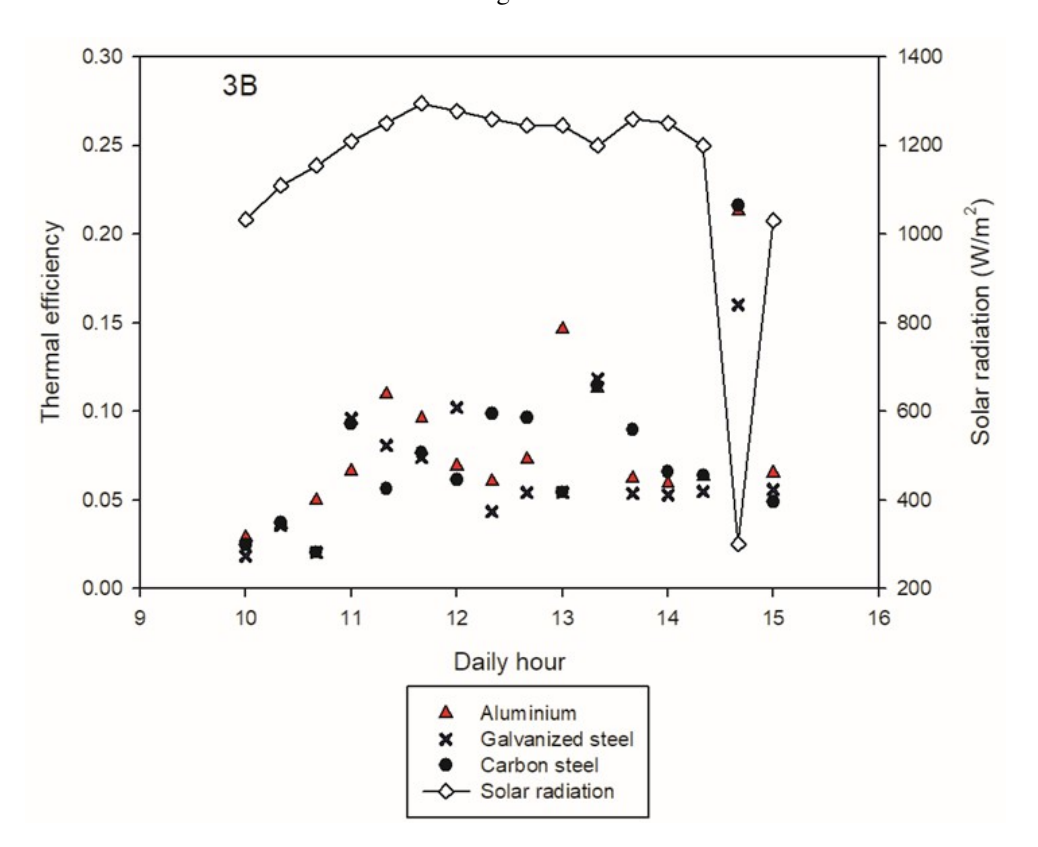


Fig. 3B.

Case II. Use of 2 sheets.

3.2 Statistical analysis

As a response variable in the experimental design, a daily overall efficiency was calculated, represented in Equation 3 (Pardeshi *et al.*, 2024). The equation represents the ratio between the total heat given up to the air and the total incident solar radiation on the plate during the experimental time. The subfix i represents the measurement periods (every 20 minutes) performed during the experiment.

$$\eta_{\text{Global}} = \frac{\sum_{i} \dot{m} C_{p} (T_{ao} - T_{ai})_{i}}{\sum_{i} (I_{\text{solar}} A_{\text{plate}})_{i}}$$
(3)

Table 1 shows the percentages of thermal efficiencies calculated according to equation 4 for the experimental design proposed 32. The efficiency data for the different materials presented in the same row were obtained by exposing the 3 SAH's to the same environmental conditions in order to reduce the experimental error. Observing the efficiency values per row shows similar values for the different materials, this also occurs when comparing the experiments with different number of sheets.

Table 2 presents the analysis of variance showing that the mean squares associated with the sources of variation of the material and the number of sheets, as well as the interaction of these materials, are lower than the experimental error. The "F" parameter and the confidence interval indicate (P) that the material and the number of sheets does not have a significant effect on the thermal efficiency of the SAH's. The parameter F is the ratio of the mean squares associated with the sources of variation studied and the mean squares associated with the experimental error; in

all cases, the error is significantly greater than the effects of the factors. (Calderón-Ramírez *et al.*, 2022) Demonstrated that environmental conditions have a substantial effect on thermal efficiencies; however, since they are considered uncontrollable factors, their effects are included in the experimental error. To avoid this situation, in this work, three identical SAHs were built to expose the different absorber plate materials to identical environmental conditions, as shown in Table 1.

3.3 Phenomenological Analysis

Figure 4 shows the air velocities at the inlet of the SAHs, measured at the center of the lower holes. It can be observed that air velocities vary significantly from their average. In general, air velocities increase with increasing solar radiation and the difference between the SAH air inlet and outlet temperatures (Figure 2). These increases are associated with free or buoyant convection mechanisms due to differences in air density as it heats towards the interior of the SAH, with a transverse contribution from temperature differences between the absorber plate and the air. In general, it is observed that the materials of the absorber plates do not affect the behavior of the air velocities. For these experiments, Grashof and Prandtl numbers were calculated to estimate the Rayleigh number. Under these conditions the Rayleigh number varies in the range of 1.07E+06 - 2.43E+06, which corresponds to a transitional laminar flow regime; to achieve the turbulent regime that satisfactorily enhances the hydrodynamic heat transfer conditions the Rayleigh number must more significant than 1.0E+09 (Sidebotham, 2015). Under these conditions, it is expected that heat transfer in the air-surface interfacial region will be limited to conduction mechanisms.

Table 1. Percentage of thermal efficiencies in SAH's

| | Material | | |
|---------|----------|------------------|--------------|
| #sheets | Aluminum | Galvanized steel | Carbon Steel |
| | 9.02 % | 8.08 % | 9.07 % |
| 1 | 5.45 % | 5.60 % | 5.59 % |
| | 7.05 % | 5.98 % | 6.59 % |
| | 5.96 % | 5.76 % | 6.20 % |
| 2 | 7.64 % | 6.35 % | 7.03 % |
| | 5.88 % | 5.87 % | 6.46 % |
| | 7.25 % | 6.79 % | 7.30 % |
| 3 | 6.22 % | 6.43 % | 6.77 % |
| | 7.65 % | 6.98 % | 7.86 % |

Table 2. Analysis of variance

| Sources of variation | Sum of squares | Degrees of freedom | Mean squares | F | Value - P |
|----------------------|----------------|--------------------|--------------|------|-----------|
| A: Material | 2.2994 | 2 | 1.1449 | 0.79 | 0.4675 |
| B: Number of sheets | 1.8552 | 2 | 0.9276 | 0.64 | 0.5389 |
| AB: Interaction | 0.1084 | 4 | 0.0271 | 0.02 | 0.9992 |
| Error | 26.0871 | 18 | 1.4492 | - | - |

www.rmiq.org 7

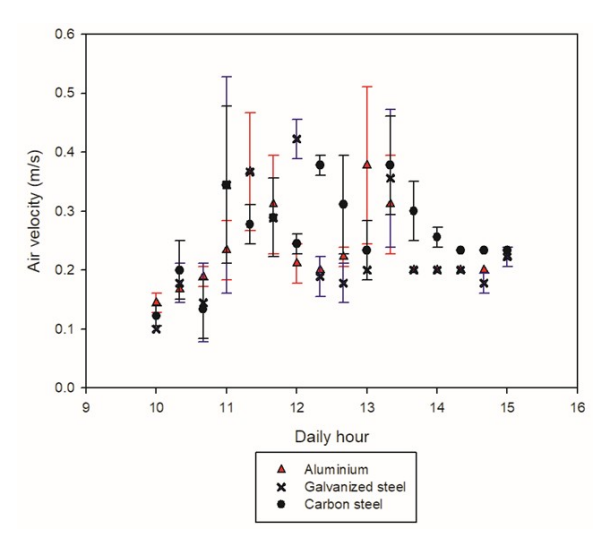


Figure 4. Average air velocities at the SAH's inlet are measured using a material plate.

Using formula (2), the convective heat coefficients between the absorber plate and the air were estimated in the range of: 4.52 - 5.82 W/m2 °C, considering the separation between the absorber plate and the glass cover as characteristic distance. Using a thermal camera, the surface temperature of the absorber plate was estimated (67.3°C - 68°C). With the temperatures at the inlet and outlet of the SAH, the average logarithmic temperature difference between the absorber plate and the air was calculated, which varied between (14.6 °C -47.7 °C). Considering the best heat transfer conditions, the plate could yield 277.61 W/m2 to the air, while the solar radiation reached up to 1400 W/m². Under this phenomenological analysis, the thermal efficiencies will not exceed 20%.

Statistical analysis of thermal efficiencies formally shows that materials and the number of layers do not have a significant effect as sources of variation. However, a deeper understanding of the experimentally observed phenomenology is needed to improve the performance of these devices. It was proposed to study heat transfer between air and the absorber plate in SAH using a composite wall model, whose overall heat transfer coefficient is expressed according to equation 3 (Yadav & Bhagoria, 2013), comprised of the resistances offered by each wall and the fluid media in contact with the external and internal surfaces of the wall.

Figure 5 illustrates a representative schematic of the absorber plate's cross-section, with the insulating material placed on its back. The heat transfer mechanisms involved are also outlined. Solar radiation is primarily absorbed at the surface of the paint film, being absorbed by the related chromophore molecules, as described by Kumar *et al.* (2022). Solar radiation causes a significant increase in molecular vibrations, which translates into an increase in the internal energy and temperature of the paint film. The other portion of solar radiation is reflected or emitted as radiation by the

black paint surface to the exterior. "In general, the direct energy interaction of solar radiation is exclusively with the surface of the paint film." Thus, the internal energy received and accumulated in the paint film is transferred to the metal plate by conduction or to the air through conduction and convection mechanisms. The rates of heat transfer to the plate or the air will depend on the local temperature gradients and the resistance offered in each area.

Table 3 presents some properties reported in the literature of the materials used. Panas *et al.*, (2021) show characteristic values of paint thicknesses and conductivities. Org (1996), show typical values of thermal conductivity of fiberglass quilts. Using the definition of overall heat transfer coefficient in composite walls shown in Equation 4 (Yadav & Bhagoria, 2013), the resistances offered by each material ($\Delta X_i/K_i$), as well as the heat transfer resistance between the absorber plate and the air ($1/h_{air-plate}$) were estimated.

$$U = \frac{1}{\frac{1}{h_{\text{air-plate}}} + \sum_{i} \frac{\Delta X_{i}}{K_{i}}}$$
 (4)

These values indicate that the heat absorbed in the paint film on the surfaces of the plates exposed to solar radiation is transferred more easily to the inside of the plate or overlapping plates than to the air flowing over the surface of the absorber plate. As can be seen, the fiberglass offers great resistance to heat loss through the bottom of the plates, and these should experience temperatures much higher than the observed values. However, it is important to establish that the temperature on the surface is controlled mainly by the heat removal capacity of the circulating air stream. Under these circumstances, it can be hypothesized that a significant portion of the heat is being reflected outward. The paint coating should have a more significant effect than the absorber plate material.

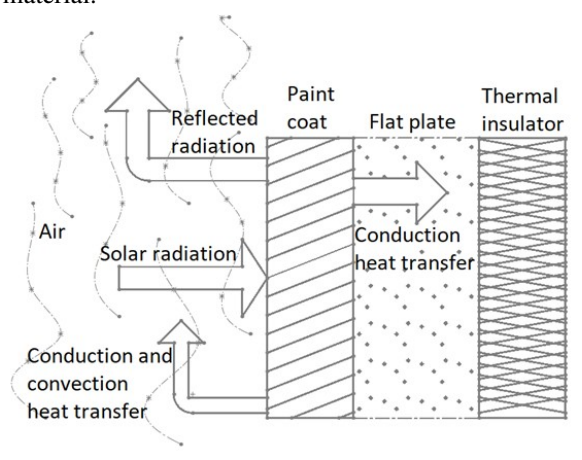


Figure 5. Composite wall model and heat transfer mechanism in the absorber plate.

Figure 3B shows that during the decrease of solar radiation due to some atmospheric effect, the efficiency of the SAH increases significantly, since the air heating does not give way even when the solar radiation decreases drastically, given that the internal energy in the absorber plate and the body of the SAH was accumulated during the time prior to the occurrence of this phenomenon. This graph shows that the aluminum plate has a much higher efficiency than the other materials. To make this phenomenon evident, experiments were carried out with intermittent exposure of the SAH to solar radiation, as described in the methodological section. Air heating rates $(\Delta T/\Delta t,$

°C/min) during exposure to solar radiation - heating and shading – cooling, were estimated. The results are presented in Table 4. The results show that the air heating or cooling rates with aluminum absorber plates are higher, mainly for the experiments with 2 and 3 plates. These results are associated with higher thermal conductivity of aluminum. These results appear to be contradictory to the analysis of variance. However, the thermal efficiency during continuous operation of a solar absorber is associated with a continuous and dynamic heat transfer process that can be disturbed circumstantially and temporarily by some uncontrolled event.

| Table 3. Thermal properties of the materials and heat transfer resistance | S |
|---|---|
|---|---|

| Materials | Specific heat (J/kg °K) | Density (kg/m ³) | Thickness (m) | Thermal conductivity (W/m °K) | Resistance (m ² °K/W) |
|------------------|-------------------------|------------------------------|-----------------------|-------------------------------|----------------------------------|
| Aluminum | 903 | 2702 | 1.5×10^{-3} | 237 | 6.32×10^{-6} |
| Carbon steel | 434 | 7854 | 1.5×10^{-3} | 60.5 | 2.47×10^{-5} |
| Galvanized steel | 444 | 7822 | 1.6×10^{-3} | 37.7 | 4.24×10^{-5} |
| Paint1 | - | - | 100×10^{-6} | 0.58 | 1.72×10^{-4} |
| Fiberglass | - | - | 3.81×10^{-2} | 0.05 | 0.762 |
| Plate - Air | - | - | _ | - | 1.71×10^{-1} |

Table 4. Heating and cooling rates of air in intermittent operation (°C/min)

| Number of plates | Aluminum | Carbon steel | Galvanized steel | | |
|------------------|----------|--------------|------------------|--|--|
| Warming up | | | | | |
| 1 | 0.2997 | 0.2912 | 0.2103 | | |
| 2 | 0.2078 | 0.1688 | 0.1078 | | |
| 3 | 0.2131 | 0.1688 | 0.1431 | | |
| Cooling | | | | | |
| 1 | -0.4656 | -0.463 | -0.2987 | | |
| 2 | -0.3775 | -0.2962 | -0.1666 | | |
| 3 | -0.4031 | -0.3132 | -0.2405 | | |

4 Conclusions

The methodological approach of constructing platforms housing several solar air heaters with different configurations allows for reducing the significant effects of weather conditions on thermal efficiency. Aluminum, galvanized steel, and carbon steel absorber plates did not show a significant difference in the air heating process in the SAH's under free convection conditions. The paint film has a controlling effect on the plate and air heating. However, experiments varying in thickness, materials, and paint treatment are needed to strengthen this conclusion and to have a better understanding of the transport phenomena occurring at the plate-air interface in solar heaters. We recommend the use of aluminum plates because of their light weight and resistance to environmental effects such as oxidation.

Acknowledgements

This work was supported by the financing of the projects: "Tecnológico Nacional de México Proyect: 20065.24P", and the acknowledgment to CONAHCYT for the scholarship granted Roberto Carlos Salmorán Salgado and Felipe de Jesús Moreno García.

References

Calderón-Ramírez, M., Gomez-Náfate, J. A., Ríos-Fuentes, B., Rico-Martínez, R., Martínez-Nolazco, J. J., & Botello-Álvarez, J. E. (2022). Analysis of the thermal efficiency of flat plate solar air heaters considering environmental conditions using artificial neural networks. Revista Mexicana de Ingeniería Química, 21(3). https://doi.org/10.24275/rmiq/Sim2833

www.rmiq.org 9

- Das, M., & Akpinar, E. K. (2020). Determination of thermal and drying performances of the solar air dryer with solar tracking system: Apple drying test. *Case Studies in Thermal Engineering*, 21. https://doi.org/10.1016/j.csite.2020.100731
- Green, D. W., & Southard, M. Z. (2019). *Perry's Chemical Engineers' Handbook*.
- Handoyo, E. A., Ichsani, D., Prabowo, & Sutardi. (2014). Experimental studies on a solar air heater having v-corrugated absorber plate with obstacles bent vertically. *Applied Mechanics and Materials*, 493, 86–92. https://doi.org/10.4028/www.scientific.net/AMM.493.86
- Kalogirou, S. (2003). The potential of solar industrial process heat applications. *Applied Energy*, 76(4), 337–361. https://doi.org/10.1016/S0306-2619(02)00176-9
- Kong, D., Wang, Y., Li, M., & Liang, J. (2024). A comprehensive review of hybrid solar dryers integrated with auxiliary energy and units for agricultural products. *Energy*, 293. https:// doi.org/10.1016/j.energy.2024.130640
- Kumar, R., Verma, S. K., Mishra, S. K., Sharma, A., Yadav, A. S., & Sharma, N. (2022). Performance Enhancement of Solar Air Heater using Graphene/Cerium Oxide and Graphene-Black Paint Coating on Roughened Absorber Plate. *International Journal of Vehicle Structures and Systems*, 14(2), 273–279. https://doi.org/10.4273/IJVSS.14.2.23
- Ladha-Sabur, A., Bakalis, S., Fryer, P. J., & Lopez-Quiroga, E. (2019). Mapping energy consumption in food manufacturing. *Trends in Food Science & Technology*, 86, 270–280. https://doi.org/10.1016/j.tifs.2019.02.034
- Iglesias-Díaz, R., Pantoja-Enriquez, J., Moreira-Acosta, J., Farrera, N., & Ibáñez-Duharte, G. (2011). Diseño de un secador solar con circulación forzada (Vol. 5, Issue 5).
- Mekhilef, S., Saidur, R., & Safari, A. (2011). A review on solar energy use in industries. *Renewable and Sustainable Energy Reviews*, *15*(4), 1777–1790. https://doi.org/10.1016/j.rser.2010.12.018
- Mohammed, S. A., Alawee, W. H., Chaichan, M. T., Abdul-Zahra, A. S., Fayad, M. A., & Aljuwaya, T. M. (2024). Optimized solar food dryer with varied air heater designs. *Case Studies in Thermal Engineering*, *53*. https://doi.org/10.1016/j.csite.2023.103961

- Org, E. (1996). Lawrence Berkeley National Laboratory Recent Work Title Impact of the Temperature Dependency of Fiberglass Insulation R-Value of Cooling Energy Use in Building Publication Date.
- Panas, A. J., Szczepaniak, R., Stryczniewicz, W., & Omen, Ł. (2021). Thermophysical properties of temperature-sensitive paint. *Materials*, *14*(8). https://doi.org/10.3390/ma14082035
- Pardeshi, P. S., Boulic, M., van Heerden, A. (Hennie), Phipps, R., & Cunningham, C. W. (2024). Review of the thermal efficiency of a tube-type solar air heaters. *Renewable and Sustainable Energy Reviews*, 199. https://doi.org/10.1016/j.rser.2024.114509
- Sanjuán, N., Stoessel, F., & Hellweg, S. (2014). Closing data gaps for LCA of food products: Estimating the energy demand of food processing. *Environmental Science & Technology*, 48(2), 1132–1140. https://doi.org/10.1021/es4033716
- Schoeneberger, C. A., McMillan, C. A., Kurup, P., Akar, S., Margolis, R., & Masanet, E. (2020). Solar for industrial process heat: A review of technologies, analysis approaches, and potential applications in the United States. *Energy*, 206. https://doi.org/10.1016/j.energy.2020.118083
- Sidebotham, G. (2015). Nusselt Number Correlations. In *Heat Transfer Modeling* (pp. 351–375). Springer International Publishing. https://doi.org/10.1007/978-3-319-14514-3_9
- Singh, I., Vardhan, S., Singh, S., & Singh, A. (2019). Experimental and CFD analysis of solar air heater duct roughened with multiple broken transverse ribs: A comparative study. *Solar Energy*, 188, 519–532.
- Srivastava, R., Kumar Rai, A., & Kumar Srivastava, R. (2017). A review on solar air heater technology. *International Journal of Mechanical Engineering and Technology*, 8(7), 1122–1131.
- Welsby, D., Price, J., Pye, S., & Ekins, P. (2021). Unextractable fossil fuels in a 1.5 °C world. *Nature*, 597(7875), 230–234. https://doi.org/10.1038/s41586-021-03821-8
- Yadav, A. S., & Bhagoria, J. L. (2013). Heat transfer and fluid flow analysis of solar air heater: A review of CFD approach. *Renewable and Sustainable Energy Reviews*, 23, 60–79. https://doi.org/10.1016/j.rser.2013.02.035